Imaging dissipation and hot spots in carbon nanotube network transistors

David Estrada[1] and Eric Pop[1,2,a)]
[1]Department of Electrical and Computer Engineering, Micro and Nanotechnology Laboratory, University of Illinois, Urbana-Champaign, Illinois 61801, USA
[2]Beckman Institute, University of Illinois, Urbana-Champaign, Illinois 61801, USA

(Received 8 October 2010; accepted 7 January 2011; published online 14 February 2011)

We use infrared thermometry of carbon nanotube network (CNN) transistors and find the formation of distinct hot spots during operation. However, the *average* CNN temperature at breakdown is significantly lower than expected from the breakdown of individual nanotubes, suggesting extremely high regions of power dissipation at the CNN junctions. Statistical analysis and comparison with a thermal model allow the estimate of an upper limit for the average tube-tube junction thermal resistance, $\sim 4.4\times 10^{11}$ K/W (thermal conductance of ~ 2.27 pW/K). These results indicate that nanotube junctions have a much greater impact on CNN transport, dissipation, and reliability than extrinsic factors such as low substrate thermal conductivity. © *2011 American Institute of Physics*. [doi:10.1063/1.3549297]

Random networks of single-walled carbon nanotubes (CNTs) are of interest for integrated circuits and display drivers[1] on flexible or transparent substrates, particularly where they could exceed the performance of organic or amorphous thin-film transistors (TFTs). Such TFTs are often placed on low thermal conductivity substrates like glass or plastics, leading to self-heating effects and reduced reliability,[2] topics not yet explored in carbon nanotube network (CNN) transistors. An additional concern with CNNs is that performance and reliability may be limited by high electrical[3] and thermal[4–7] intertube junction resistances. For CNNs, this could result in large temperature increases (hot spots) at the CNT junctions, which greatly exceed the average temperature of the device.

In this study, we use infrared (IR) thermal imaging[8] and electrical breakdown thermometry[9] to investigate power dissipation in CNNs. We show that under voltage stress, devices fail with a minimal rise in *average* temperature. Furthermore, we find that power dissipation can be localized at "hot spots" in the CNN, which can be detrimental to TFT applications. We also introduce a model to extract the average thermal resistance between CNNs and the substrate (R_C), as well as the CNT junction thermal resistance (R_J). Our results indicate that the latter is the key limiting factor in CNN performance, dissipation, and reliability.

The CNN devices in this work are networks of single-walled CNTs fabricated on SiO_2(90 nm)/Si substrates, as outlined in the supplementary information[10] and shown in Fig. 1. All IR thermometry is performed at a background temperature $T_0=70$ °C for optimum IR microscope sensitivity.[8] The highly n-doped Si acts as a back gate, set to $V_G<-15$ V here, such that both metallic and semiconducting CNTs are "on." We acquire IR images at increasing source-drain bias (V_{SD}) and, surprisingly, we find that the imaged channel temperature increases very little, even near the device breakdown. For instance, the maximum temperature rise imaged[10] in the high density[11] (HD) CNN shown in Fig. 1 is $\Delta T \approx 108$ °C at a power $P=I_D V_{SD}=25$ mW. Moreover, the temperature in the channel is nonuniform, with distinct hot spots, which depend on the local CNN density variations and the CNT percolative pathways.

Lower density (LD) CNNs [Fig. 2(a)] do not provide as strong an IR thermal signal,[10] but facilitate analysis as the number of CNT junctions can be examined and counted by scanning electron microscopy (SEM),[11] as shown below. The measured power versus voltage of LD and HD CNNs up to breakdown (BD) are shown in Fig. 2(b). For both, we note a sharp and irreversible drop, corresponding to $P_{BD}\sim 6.7$ and 30 mW for the LD and HD devices, respectively. This signals a catastrophic break of the CNN, also noted when the LD device cannot be recovered on a subsequent sweep [dashed line in Fig. 2(b)]. In addition, the breakdown location of the film from Fig. 2(c) bears the imprint of the hot spot formation in the overlaid image of Fig. 2(d).

We now focus on the LD device to understand how P_{BD} corresponds to T_{BD} and the temperature measured by IR mi-

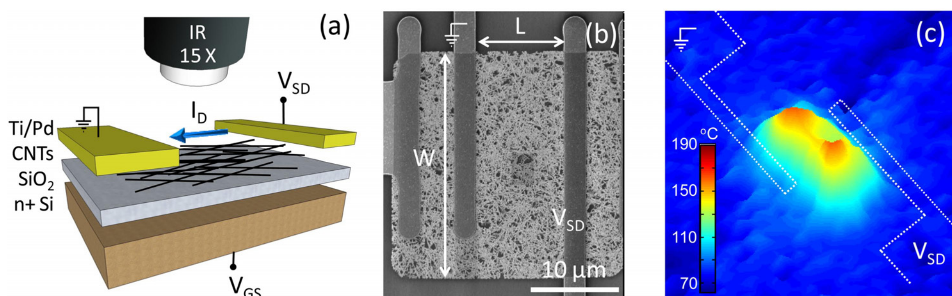

FIG. 1. (Color online) (a) Schematic of the CNN device and experimental setup. (b) SEM of high density (HD) CNN ($W/L \approx 25/10$ μm) before IR imaging and CNT breakdown. (c) Temperature of the device in (b) measured at $P\approx 25$ mW, in air, with $T_0=70$ °C (Ref. 10). The nonuniform temperature profile is indicative of percolative transport in such CNNs.

a)Electronic mail: epop@illinois.edu.

 © 2011 American Institute of Physics

Author complimentary copy. Redistribution subject to AIP license or copyright, see http://apl.aip.org/apl/copyright.jsp

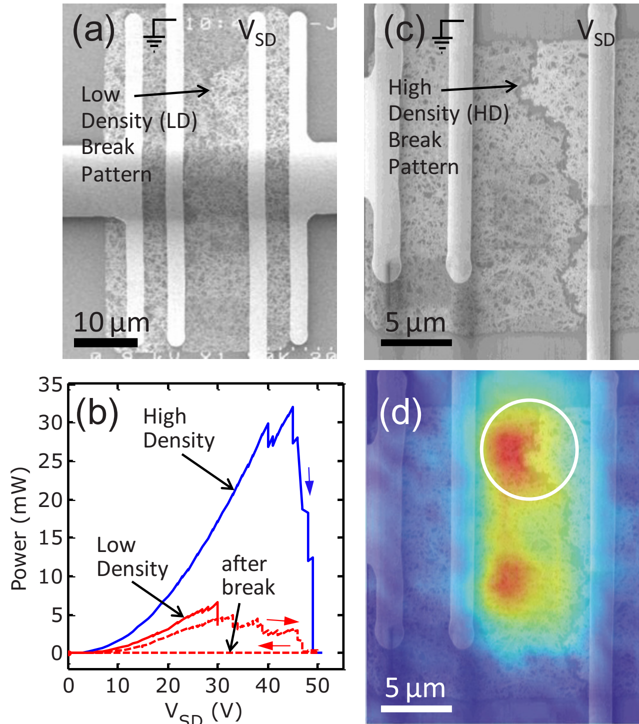

FIG. 2. (Color online) (a) SEM image of the LD device ($W/L \approx 50/10$ μm). (b) Measured power vs voltage up to breakdown of the LD device from (a) and HD device from (c). In both cases, large drops in power mark breaking of the CNN. The dashed line shows a second sweep of the LD device, taken after the first test was stopped at $V_{SD}=30$ V break. Small arrows indicate sweep directions. (c) SEM image of the HD device from Fig. 1(b) after breakdown. (d) Measured temperature just before breakdown, at $P=25$ mW from Fig. 1(c), overlaid onto the SEM from (c). The circled breakdown location bears the imprint of the adjacent hot spot. Although the breakdown occurs too fast to be imaged by the IR camera, we suspect that the initial CNN break occurred at the upper hot spot, leading to a rerouting of the current pathways to cause the subsequent full break.

croscopy. In general, the power and temperature rise of a device are related through its thermal resistance,[12] here $T_{BD} - T_0 = P_{BD} R_{TH}$ at breakdown. We develop a thermal resistance model, as shown in Fig. 3(a), and we assume the well-known $T_{BD}=600$ °C for CNTs in air,[9] recalling that $T_0 = 70$ °C. To simplify the analysis, we assume uniform power dissipation across the CNN, although this is not strictly the case due to the percolative transport, as well as the imaged temperature profile [Fig. 2(d)]. However, as we will show, this allows us to determine a quantitative upper bound on the CNT junction resistance, R_J.

We note that power is dissipated both at the CNT junctions and along the length of the CNTs in contact with SiO_2.[13] This requires knowledge of the junction area fill factor (γ_J) with respect to the CNN area (A_C). To determine γ_J, we first extract the area fill factor of the network (γ_C) by analyzing SEM images. The images are imported to a matrix form in MATLAB (Ref. 14) and a threshold contrast is chosen to designate areas occupied by CNTs,[10] as shown in Fig. 3(b). The proportion of matrix elements with values above threshold is ~0.72, which is a significant overestimate of the true areal coverage (γ_C) as CNT diameters appear much larger under SEM, $30 < \langle d' \rangle < 80$ nm. Choosing $\langle d' \rangle \approx 50$ nm, we estimate the total length of CNTs in the network, $L_C \approx 7.2$ mm, from $\gamma_C = \langle d' \rangle \Sigma L_C / A$, where the device area is $A=WL$. The actual area of the CNN is $A_C \approx dL_C \approx 14.4$ μm^2, with a true device area fill factor $\gamma_C \approx 0.03$, where $d \approx 2$ nm is the real CNT diameter averaged from atomic force microscopy analysis. (We return to the effect of variability introduced by the SEM analysis below.)

We estimate the total CNT-CNT junction area as $A_{J\,tot} \approx A_J(n_J A)$, where A_J is the average area of a CNT junction and n_J is the junction density per device area A. We note that the junction area depends on the angle of intersection (θ) of CNTs in the random network, i.e., $A_J = d^2/\sin(\theta)$. Here, we again use image analysis software[14] to determine average values for n_J, A_J, and θ, as shown by histograms in Fig. 3(c). We find $A_J = 4.69 \pm 0.93$ nm^2, $\theta = 98 \pm 28°$, and $n_J \approx 26$ μm^{-2}. Thus, the density of junctions in the network $\gamma_J = A_{J\,tot}/A_C = 0.0042$, which completes the inputs needed for the thermal model in Fig. 3(a). We note that, in general,[3] n_J will be proportional to CNN density and inversely proportional with CNT segment lengths[13] between junctions. Therefore, when modeling other devices, it is important to carefully estimate n_J for the particular CNN.

To find the total thermal resistance[12] of the CNN, we include the Si substrate thermal resistance $R_{Si} = 1/(2\kappa_{Si} A^{1/2})$, the SiO_2 thermal resistance $R_{ox} = t_{ox}/(\kappa_{ox} A_C)$, and the CNT-$SiO_2$ thermal boundary resistance of the network $R_C = 1/(g L_C)$. Here, $t_{ox}=90$ nm, $\kappa_{ox} \approx 1.4$ W m^{-1} K^{-1}, $\kappa_{Si} \approx 100$ W m^{-1} K^{-1}, and $g \approx 0.3$ W K^{-1} m^{-1} for CNTs with a diameter of ~2 nm near breakdown.[9] This gives $R_{Si} = 223.6$ K W^{-1}, $R_{ox} = 4.46 \times 10^3$ K W^{-1}, and $R_C = 462.9$ K W^{-1}, respectively.

We can now calculate the temperature rise at the SiO_2–Si interface, $\Delta T_{Si} = T_{Si} - T_0 = P_{BD} R_{Si} \approx 1.5$ K. This is a good match with the temperature measured by IR

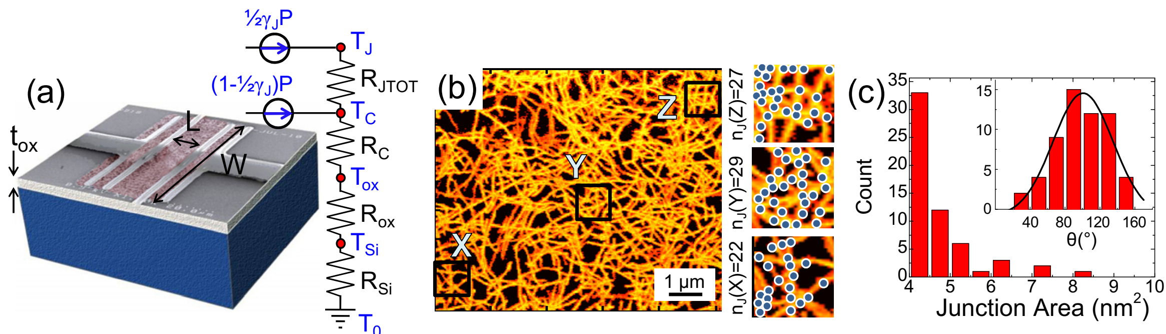

FIG. 3. (Color online) (a) Thermal resistance model used to evaluate CNN dissipation and estimate the temperature differences, including from CNT junctions. (b) Processed SEM image of part of the LD device [from Fig. 2(a)] used for analysis of the total CNN length (L_C), area (A_C), and junction density (n_J). Highlighted portions of the SEM are magnified and the number of CNT junctions (dots) is counted to obtain averages. (c) Histogram of the average CNT junction area A_J and (inset) angle of intersection θ.

Author complimentary copy. Redistribution subject to AIP license or copyright, see http://apl.aip.org/apl/copyright.jsp

imaging for this device, considering that most of the IR signal originates from the top of the heated Si substrate.[8,10] The temperature drop across SiO_2 is $\Delta T_{ox}=T_{ox}-T_{Si}=P_{BD}R_{ox}\approx 29.9$ K, and the temperature drop across the CNT-SiO_2 interface is[15] $\Delta T_C=T_C-T_{ox}=(1-\gamma_J/2)P_{BD}R_C\approx P_{BD}R_C=3.1$ K. Thus, the average temperature of the CNN *without* considering the effect of the junctions is merely $T_C\approx 104.5$ °C, much smaller than the breakdown temperature of CNTs in air, $T_{BD}\approx 600$ °C. This remains the case even when variability of the CNT-SiO_2 thermal coupling[9] (g) and that of the apparent diameter in SEM $\langle d'\rangle$ are taken into account. In other words, considering $g=0.3\pm 0.2$ W K^{-1} m^{-1} and $30<\langle d'\rangle<80$ nm in our analysis leads to a range $T_C\approx 90-135$ °C.

We suggest that the "missing" temperature difference is due to highly localized hot spots associated with the CNT junctions, which cannot be directly visualized by the IR thermometry. This is consistent with the emerging picture of CNT junctions being points of high electrical[3] and thermal[4–7] resistance. Consequently, we can extract the thermal resistance of all CNT junctions ($R_{J\,\mathrm{tot}}$) in the network acting in parallel,[15]

$$R_{J\,\mathrm{tot}}=\frac{T_{BD}-T_C}{1/2\gamma_J P_{BD}}=\frac{T_{BD}-\Delta T_C-\Delta T_{ox}-\Delta T_{Si}-T_0}{1/2\gamma_J P_{BD}}, \quad (1)$$

which is bound between 2.1×10^7 and 5.9×10^7 K W^{-1} when allowing for uncertainty in g and $\langle d'\rangle$ as above. $R_{J\,\mathrm{tot}}$ is several orders of magnitude greater than any other thermal resistance in the network and remains dominant even if the SiO_2 were replaced with a substrate ten times less thermally conducting (e.g., plastics). If substrates with much higher thermal conductivity than SiO_2 are used (e.g., sapphire), the CNN junction thermal resistance will be even more of a limiting factor for dissipation and reliability.

We now estimate the thermal resistance of a single CNT junction as $R_J\approx R_{J\,\mathrm{tot}}(n_J A)\approx 4.4\times 10^{11}$ K W^{-1}, equivalent to a thermal conductance $G_J\approx 2.27$ pW K^{-1}. We note it is likely that not all counted CNT junctions conduct current despite our effort to deliberately gate (turn on) the semiconducting CNTs. Thus, our estimate of CNT junction thermal resistance (conductance) represents an upper (lower) limit. Furthermore, accounting for the variability in CNT-SiO_2 coupling and $\langle d'\rangle$ from SEM analysis, we can place bounds on our estimate, $R_J\approx(2.7-7.6)\times 10^{11}$ K W^{-1} ($G_J\approx 1.3-3.6$ pW K^{-1}). The R_J obtained here is in good agreement with experimental results for bulk *single-walled* CNTs,[6] $\sim 3.3\times 10^{11}$ K W^{-1}, and is one order of magnitude greater than measurements of intersecting *multi-walled* CNTs,[7] as would be expected. Our average CNT junction thermal resistance normalized by the average contact area from Fig. 3(c) is $r_J\approx 2.1\times 10^{-6}$ m^2 K W^{-1}. This is one order of magnitude greater than $\sim 10^{-7}$ m^2 K W^{-1} predicted by molecular dynamics simulations for overlapping (10,10) CNTs with 3.4 Å separation,[4,6] perhaps due to idealized conditions in the simulation or imperfection in the experiments.

To further understand the large apparent thermal resistance at the CNT junctions, we note that this is not only a function of the small overlap area A_J but also of the average CNT separation and van der Waals interaction.[4,6] In the harmonic approximation, the spring constant between pairs of atoms is $K=72\varepsilon/(2^{1/3}\sigma^2)$ from a simplified Lennard-Jones 6-12 potential,[16] where ε is related to the depth of the potential well and σ is a length parameter. Using typical parameters,[9,17] we find $K_{C\text{-}C}<K_{C\text{-ox}}/2$, i.e., the CNT-CNT thermal coupling is weaker than the CNT-SiO_2 thermal coupling per pair of atoms. This simple analysis does not account for the exact shape of the CNTs[9,17] or the role of SiO_2 surface roughness,[9] and thus further work must consider these effects to investigate the relatively "high" experimentally observed thermal resistance at single-walled CNT junctions.

In conclusion, we directly imaged power dissipation in CNN transistors using IR microscopy. We found that local hot spots in power dissipation detected by IR correlate with the subsequent breakdown of the network mapped by SEM. Nevertheless, these hot spots do not account for the CNN breakdown at relatively low *average* temperatures, <180 °C. Instead, our analysis suggests that CNN breakdown occurs at highly resistive CNT-CNT junctions, allowing us to extract the junction thermal resistance $R_J\approx 4.4\times 10^{11}$ K W^{-1} (conductance of 2.27 pW K^{-1}). These findings suggest that transport, dissipation, and reliability of CNNs are limited by the CNT junctions rather than extrinsic factors such as low substrate thermal conductivity.

We acknowledge the support from NSF Grant CAREER ECCS 0954423, the NRI through the Nano-CEMMS Center, the Micron Technology Foundation, and the NDSEG Fellowship. We are indebted to A. Liao, J. D. Wood, and Z.-Y. Ong for helpful discussions and technical support.

[1] Q. Cao, H.-s. Kim, N. Pimparkar, J. P. Kulkarni, C. Wang, M. Shim, K. Roy, M. A. Alam, and J. A. Rogers, Nature (London) **454**, 495 (2008); S. Kim, S. Kim, J. Park, S. Ju, and S. Mohammadi, ACS Nano **4**, 2994 (2010).
[2] A. Valletta, A. Moroni, L. Mariucci, A. Bonfiglietti, and G. Fortunato, Appl. Phys. Lett. **89**, 093509 (2006); K. Takechi, M. Nakata, H. Kanoh, S. Otsuki, and S. Kaneko, IEEE Trans. Electron Devices **53**, 251 (2006).
[3] L. Hu, D. S. Hecht, and G. Gruner, Nano Lett. **4**, 2513 (2004); S. Kumar, J. Y. Murthy, and M. A. Alam, Phys. Rev. Lett. **95**, 066802 (2005); P. E. Lyons, S. De, F. Blighe, V. Nicolosi, L. F. C. Pereira, M. S. Ferreira, and J. N. Coleman, J. Appl. Phys. **104**, 044302 (2008); P. N. Nirmalraj, P. E. Lyons, S. De, J. N. Coleman, and J. J. Boland, Nano Lett. **9**, 3890 (2009).
[4] H. Zhong and J. R. Lukes, Phys. Rev. B **74**, 125403 (2006).
[5] S. Kumar, M. A. Alam, and J. Y. Murthy, Appl. Phys. Lett. **90**, 104105 (2007).
[6] R. S. Prasher, X. J. Hu, Y. Chalopin, N. Mingo, K. Lofgreen, S. Volz, F. Cleri, and P. Keblinski, Phys. Rev. Lett. **102**, 105901 (2009).
[7] J. Yang, S. Waltermire, Y. Chen, A. A. Zinn, T. T. Xu, and D. Li, Appl. Phys. Lett. **96**, 023109 (2010).
[8] M.-H. Bae, Z.-Y. Ong, D. Estrada, and E. Pop, Nano Lett. **10**, 4787 (2010).
[9] A. Liao, R. Alizadegan, Z.-Y. Ong, S. Dutta, F. Xiong, K. J. Hsia, and E. Pop, Phys. Rev. B **82**, 205406 (2010).
[10] See supplementary material at http://dx.doi.org/10.1063/1.3549297 for fabrication details, IR measurement calibration, and image analysis.
[11] We label networks as HD if they are too dense to image individual CNTs by SEM. HD devices also carry much higher current density [Fig. 2(b)], here >10 times than LD devices (note the two times difference in width).
[12] E. Pop, Nano Res. **3**, 147 (2010).
[13] We estimate the average CNT length between junctions as $L_{link}\sim L_C/(4An_J)\sim 0.3$ μm, in good agreement with imaging in Fig. 3. Transport is diffusive in such links, which are much longer than the high-field mean free path [~30 nm, see, e.g., A. Liao, Y. Zhao, and E. Pop, Phys. Rev. Lett. **101**, 256804 (2008)].
[14] MATLAB, http://mathworks.com.; GWYDDION, http://gwyddion.net.
[15] The $1/2\gamma_J$ term is the fraction of power dissipated at the junctions versus the total power dissipated in the entire network.
[16] R. Prasher, Appl. Phys. Lett. **94**, 041905 (2009).
[17] Z.-Y. Ong and E. Pop, Phys. Rev. B **81**, 155408 (2010).

Author complimentary copy. Redistribution subject to AIP license or copyright, see http://apl.aip.org/apl/copyright.jsp

Supporting Online Materials for "Imaging Dissipation and Hot Spots in Carbon Nanotube Network Transistors" by D. Estrada, and E. Pop, University of Illinois, Urbana-Champaign, U.S.A. (2011)

1. Carbon nanotube network (CNN) device fabrication: CNN devices used in this study were grown using an Etamota chemical vapor deposition (CVD) system. Low density devices were fabricated with ferritin catalyst following [SR-1]. High density devices were made by depositing ~2 Å Fe catalyst by e-beam evaporation. In both cases the catalysts were placed onto 90 nm SiO_2 on highly n-doped Si which acts as a back gate. Substrates were annealed at 900 °C in an Ar environment, followed by CNT growth for 15 minutes under CH_4 and H_2 flow. Standard photolithographic techniques were used to pattern the CNN by oxygen plasma etching, and the electrodes (Ti/Pd 1/40 nm) by lift-off, as shown in Fig. 1. Electrical and thermal measurements were performed using a Keithley 2612 dual channel source-meter and a QFI InfraScope II infrared (IR) microscope, respectively.

2. Infrared Measurement Technique: Before performing IR measurements of the CNN-TFTs, we acquire a reference radiance image which is used to calculate the emissivity at each detector pixel. This is done without biasing the device, at a background temperature T_0 ~ 70 ^oC for optimum IR microscope sensitivity [SR-2]. We then measure the background temperature with the IR scope to confirm the setup, verifying all pixels measure T_0.

3. Infrared Properties of SiO_2 and Real Temperature of CNT junctions: We can assume the SiO_2 is effectively transparent for near-IR radiation, because the thickness of the SiO_2 layer (90 nm) is much less than the optical depth for SiO_2 at these wavelengths. The optical depth for highly doped Si is much smaller and the temperature in the Si is highest near the Si-SiO_2 interface [SR-2; SR-3]. Hence, the IR Scope is effectively reading a thermal signal corresponding to a combination of the CNN temperature and that of the Si substrate near the Si-SiO_2 interface [SR-3].

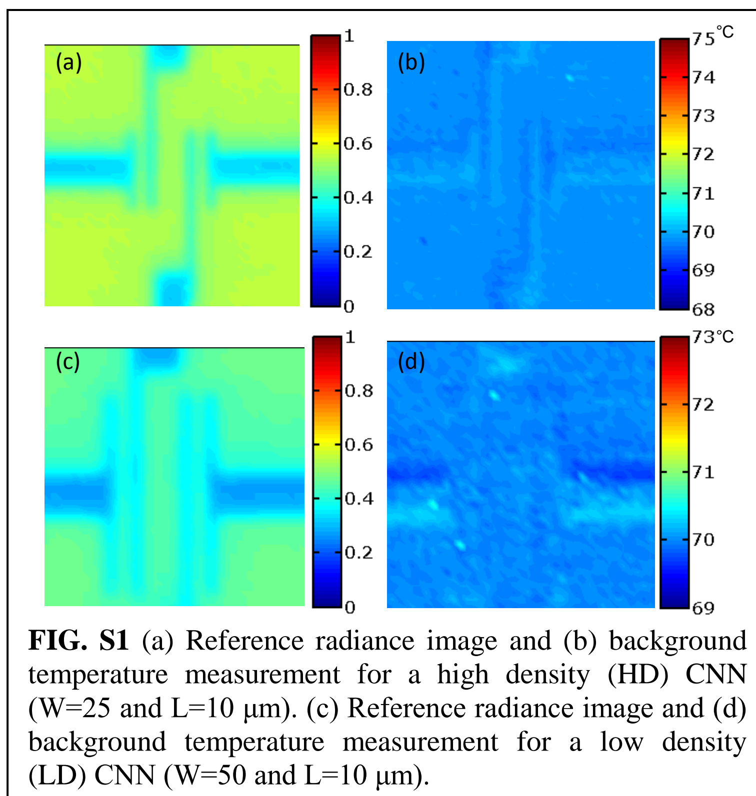

FIG. S1 (a) Reference radiance image and (b) background temperature measurement for a high density (HD) CNN (W=25 and L=10 μm). (c) Reference radiance image and (d) background temperature measurement for a low density (LD) CNN (W=50 and L=10 μm).

To estimate the average temperature of the CNN given the temperature reported by the IR scope, we follow [SR-2] and the model in Fig. 3(a) in our main text. Thus, $(T_C\text{-}T_0) = (T_{Si}\text{-}T_0)(R_C+R_{ox}+R_{Si})/R_{Si}$.

Similarly, we can estimate the ratio between the T rise of the CNT junctions in the LD device and that of the Si surface as $(T_J\text{-}T_0)/(T_{Si}\text{-}T_0) = ½\,\gamma_J(R_{JTOT}+R_C+R_{ox})/R_{Si} \approx 326.$

This agrees well with the imaged T profile of the LD device in Fig. S2. Here, the imaged temperature rise is only 1.5 °C. The actual temperature of the junctions near the breakdown power is nearly ~560 °C, consistent with the breakdown temperature of CNTs in air (see main text).

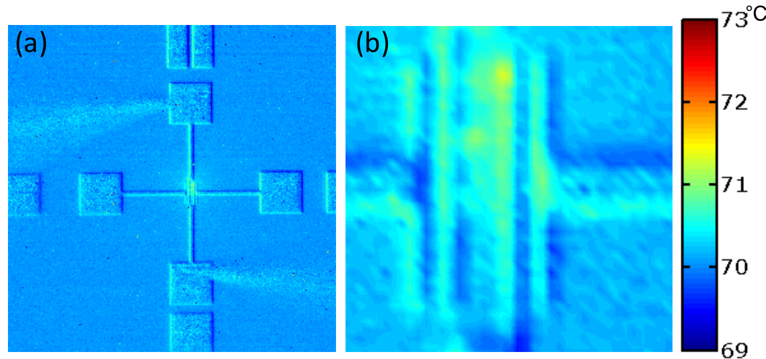

FIG. S2 (a,b) Temperature profile of the low-density (LD) device in Fig. S1(c-d) taken at a power of ≈ 5 mW and a background temperature $T_0 = 70$ °C. The non-uniform temperature profile is indicative of percolative transport in CNT devices.

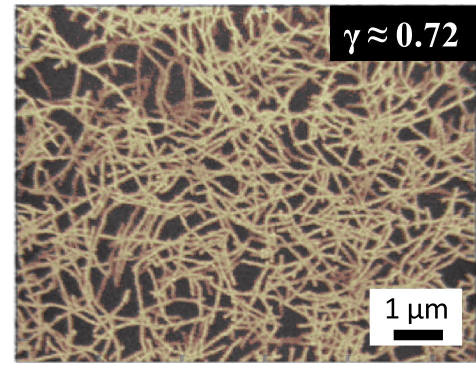

FIG. S3 (a) Overlay of raw SEM data from Fig. 3(c) and Matlab modified SEM image, as used for analysis of the CNN length (L_C), area (A_C), and junction density (n_J). The apparent CNN area fill factor is ~0.72, which is an over-estimate due to the large apparent CNT diameter under SEM. The actual area fill factor for this network was closer to $\gamma_C = 0.03$ (see main text).

<u>4. Temperature Estimate of HD CNN:</u> While the temperature estimates of the LD CNN are given with comprehensive detail in the main text, this is not immediately possible for the HD CNN because the number of junctions and CNTs are not as easily countable. Nevertheless, to obtain the true temperature rise in Figs. 1(c) and 2(d) we perform the following estimate. Since the current of the HD device is ~5x that of the LD device, but their electrode separation is the same (10 µm), we surmise that $L_{C,HD} \sim 5L_{C,LD} \sim 36$ mm. On the other hand, we note that the area of the HD device, $A_{HD} \sim A_{LD}/2 \sim 250$ µm^2. Thus, from the (more exact) LD device thermal resistances obtained in the main text, we estimate the same for the HD device as: $R_{C,HD} \sim R_{C,LD}/5 \sim 93$ K/W, $R_{ox,HD} \sim R_{ox,LD}/5 \sim 892$ K/W and $R_{Si,HD} \sim \sqrt{2}R_{Si,LD} \sim 317$ K/W.

From these, we obtain the ratio between the T rise of the HD CNN vs. that imaged by IR is $(T_C\text{-}T_0) = (T_{Si}\text{-}T_0)(R_C+R_{ox}+R_{Si})/R_{Si} \sim 4.1$. Thus, since the peak T rise measured by IR for the HD CNN is ~ 26.3 K, the true peak temperature rise of the HD CNN is $\Delta T_{HD} \sim 108$ K (main text, page 1), or a maximum temperature $T_{HD} \sim 70 + 108 \sim 178$ °C [main text, Figs. 1(c) and 2(d)].

<u>Supplementary References:</u>

[SR-1] S.-H. Hur, C. Kocabas, A. Gaur, O.O. Park, M. Shim, and J.A. Rogers, *Journal of Applied Physics* **98**, 114302 (2005).
[SR-2] M.-H. Bae, Z.-Y. Ong, D. Estrada and E. Pop, *Nano Letters* **10**, 4787 (2010).
[SR-3] H. R. Philipp, *Journal of Physics and Chemistry of Solids* **32**, 1935 (1971).